

# WBAN BASED PROTOTYPE FOR ACTIVE BODY CLIMATE CONTROL BASED ON ENVIRONMENTAL AND INDIVIDUAL SENSOR DATA

A. Gharbi, M. Breuel, W. Darmoul, W. Stork, K. D. Mueller-Glaser

*Institute for Information Processing Technology, Karlsruhe Institute of Technology (KIT), Karlsruhe, Germany*

S. Heuer

*FZI (Research Center for Information Technology), Karlsruhe, Germany*

S. Haertel

*Institute of Sports and Sport Science, Karlsruhe Institute of Technology (KIT), Karlsruhe, Germany*

**Keywords:** Wireless body area network, Vital parameters monitoring, Active body climate control, Energy expenditure, Regulation algorithm.

**Abstract:** In this paper, a new textile integrated WBAN based prototype for active body climate control is presented. The design of this prototype resulted from a previous evaluation system, which has been tested in a field study. In addition, new algorithms for determining the metabolic activity from measured vital parameters (heart rate and activity) and thus controlling the cooling mechanism by setting the necessary ventilation airflow have been conceived. A field study involving nine test persons has been conducted in order to test the new prototype and validate the conceived algorithms.

## 1 INTRODUCTION

Nowadays, the need for a local textile integrated active body climate control is getting more and more important and essential. In fact, a system that offers such functionality could relieve staff like rescue personnel and special police units that have to wear protective clothing (in this use case ballistic garments). This type of clothing leads, even undesired, to a thermal isolation, which prevents the wearer from dissipating the generated body heat that varies between 80% and 100% of the total metabolic activity of the body (Silbernagl and Despopoulos, 2003; Fiala et al., 1999). In this way, the thermal load increases very fast with an increase in the metabolic activity and the body can overheat. Consequently, this leads to a decrease in physical performance and thermal comfort and thus to a limitation of the working time.

Another target group, which could benefit from such a system, are the elderly, who have cardiovascular problems. These people cannot stand excessive heat that could lead to a collapse of their cardiovascular system, if their physiological thermoregulation

mechanisms do not get active support by adjusting the climate of their surroundings. This could be achieved by either controlling the room temperature by air conditioners or by varying the amount of air circulating in the vicinity of their skin surface, which could be realized by a textile integrated active body climate control system.

The latter is primarily a cooling system that is meant to support the heat exchange mechanisms of the body by improving the convection and especially the evaporation. For instance, the evaporation of 1 liter of sweat could take around 2400 kJ (equivalent to 667 Wh) away from the body. This approximately corresponds to a physical power dissipation of 100 W (in form of body heat) during 6.7 hours. An airflow of 100 L/min having a temperature of 30°C and a relative humidity of 20% (thus able to transport 24 g/m<sup>3</sup> of water) could theoretically transport the generated heat away from the body.

The climate control system should therefore get an input from several vital and environmental parameters in order to identify the cooling needs of the user.

Another aspect of utmost importance is that such

a system could play a major role in energy saving. In fact, the active body climate control system not only offers the advantage of portability but also needs only about 2 to 3 W of electrical power (primarily for the integrated ventilators), which corresponds to about 0.1% of the energy consumed by a commercial room air conditioner.

## 2 METHODS AND MATERIALS

After the implementation of a first prototype for an active body climate control system and the conduction of a field study (Gharbi et al., 2010), several enhancements concerning system concept, design issues, textile integration and body climate regulation algorithm have been carried out. Consequently, a second generation prototype has been realized and a second field study, similar to the first one, was conducted in order to collect feedback information from the users and to validate the reliability of the sensor data and the conceived algorithms.

### 2.1 Prototype

In this section, the realized prototype is described. As Figure 1 shows, the prototype comprises three main components; a sensor shirt, a cooling vest (worn on the sensor shirt) and a user feedback terminal (in this case a PDA). These components build up a wireless body area network (WBAN) by means of two wireless technologies. The first wireless technology uses the low power radio modules iM221A from IMST for the 2.4 GHz ISM band (IMST GmbH, 2009). These assure the data exchange between the sensor shirt and the cooling vest. In order to exchange data between the cooling vest and the PDA, a Bluetooth module (MITSUMI WML-C46) (MITSUMI ELECTRIC CO., LTD., 2010) has been integrated into the control board of the cooling vest. Through that channel, data can be bidirectionally transmitted for different purposes like online visualization of the sensor data and the calculated body heat and ventilation level, input of user specific data like weight, height and age into the system, and user feedback that adjusts the determined ventilation level in the cooling vest. Both control boards of the sensor shirt and the cooling vest integrate a 16 bit RISC microcontroller from the PIC24FJ256GB110 family (Microchip Technology Inc., 2010).

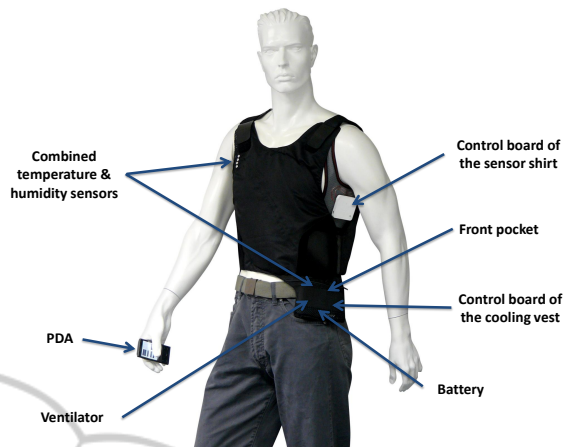


Figure 1: The new prototype for active body climate control.

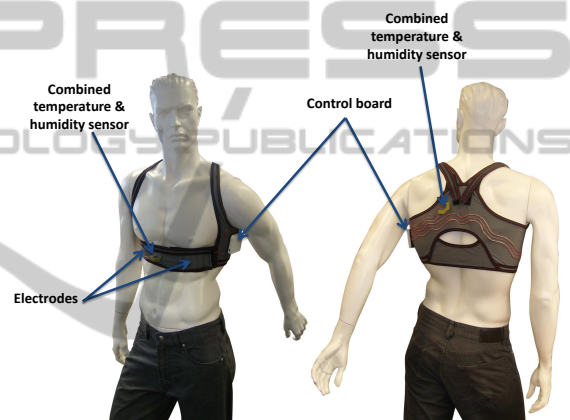


Figure 2: The sensor shirt component.

#### 2.1.1 Sensor Shirt

The sensor shirt, as shown in Figure 3, is made of an elastic material permeable to moisture, which fits the body form and lets the generated evaporation heat of the body diffuse towards the ventilation layer of the cooling vest. It also integrates several sensors and a control board in order to determine the actual body climate and its energy expenditure due to physical activity. These modules can be attached to the textile via snap fasteners.

The sensor shirt includes the following vital parameter sensors:

Two combined sensors for measuring temperature and relative humidity (temperature compensated) are used in the area of the chest and the upper back due to the non uniform distribution of the skin temperature (Fiala et al., 1999; Olesen and Fanger, 1973; Crawshaw et al., 1975). The relative humidity at the skin surface is besides a good index for determining the

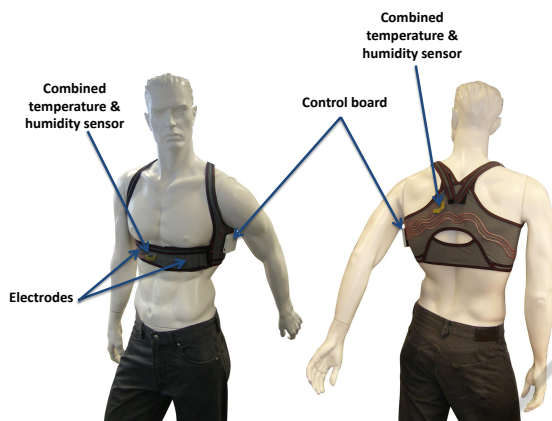


Figure 3: The sensor shirt component.

amount of heat losses in form of evaporation. The latter represents the largest part of the body heat given up to the surroundings and especially at high surroundings temperature and/or metabolic activity.

In order to detect the heart rate, two conductive rubber based ECG electrodes are integrated into the shirt. An analog front-end module, which is part of the control board, detects the QRS complexes in the ECG signal and generates digital square pulses at each QRS event. This digital signal is connected to an input capture module of the microcontroller, which enables the calculation of the heart rate. To get an ECG signal of a good quality, the crossover impedance between the skin surface and the electrodes has to be very low. In the case of sport activity, the fast formation of a sweat film under the electrodes decreases the crossover impedance. In the conducted field study, a cream for ECG electrodes is applied.

Additionally, a 3D acceleration sensor is integrated into the control board. From the measured acceleration data, the Activity Equivalent ACceleration (*AEAC*) can be calculated according to the equations 1 and 2 (Gharbi et al., 2010). Thereby, *EEAC* stands for Energy Equivalent ACceleration and represents the signal energy from all three axes together averaged in a time period of one second (Jatob et al., 2007).  $f_s$  denotes the sampling rate of the acceleration data (in the current system 20 Hz).

$$AEAC = |(EEAC - 1)| \quad (1)$$

$$EEAC = \frac{1}{f_s} \sum_{i=1}^{f_s} \sqrt{a_{xi}^2 + a_{yi}^2 + a_{zi}^2} \quad (2)$$

### 2.1.2 Cooling Vest

The cooling vest is worn over the sensor shirt and integrates a 7 mm thick space holder material, through which fresh air can circulate, and has a total weight of

approximately 680 g. It has two different ventilation parts for separate control of the body climate at the chest and the back area. These are assembled to each other via velcro fastener. As Figure 4 shows, each ventilation part has an air inlet in the top left corner and an air outlet in the opposite bottom right corner, where a ventilator is placed in order to aspirate the air and thus lead to the circulation of the air over the upper part of the body. In this way, the air blown out at the outlet becomes warmer and more humid due to the released body heat via evaporation and convection.

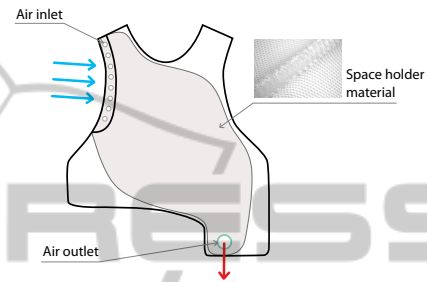


Figure 4: Design of the ventilation area of the cooling vest.

Thereby, the inner textile separation layer is, unlike the outer one, permeable to the moisture. In addition, each ventilation part of the cooling vest integrates two combined sensors for measuring temperature and relative humidity at both the inlet and the outlet. These latter can be used to monitor the ambient air (from the sensor at the inlet) and the thermal exchange between the body surface under the vest and the circulating air in the vest (from the sensor at the outlet). Each ventilation part of the cooling vest also has a pocket (see Figure 1), where a radial ventilator that allows an airflow up to 50 L/min and a rechargeable lithium-polymer battery (7.4 volt and a capacity of 1100 mAh), which allows an operating time of more than 7 hours for the ventilator at full performance, are placed. The applied voltage to both of the ventilators is controlled by a PWM modulator on the control board, which is placed in the front pocket (see Figure 1). As a result, the ventilation level in the vest can be changed according to the current level of the regulation algorithm and a maximal total airflow of around 100 L/min can be set.

This control board represents the main node of the system, where the management of the wireless communication with the other slaves (sensor shirt and PDA), the signal processing, the climate regulation algorithm and the ventilation control take place. It also integrates an SDHC memory card in order to save all sensor and regulation algorithm data for offline analysis.

### 2.1.3 Feedback Interface: PDA

The PDA communicates with the control board of the cooling vest via Bluetooth. On the one hand, it gives the user the possibility to change the ventilation level according to his individual preferences. On the other hand, it allows the online visualization of all vital and system parameters.

### 2.1.4 Textile Integration

All electronic modules of the different system components, whether small sensor modules (for instance the modules of the combined temperature and humidity sensors) or control boards of both the sensor shirt and the cooling vest, have snap fastener (like Figure 5 shows) and can be thus detached from the textile material, when the latter needs to be washed.

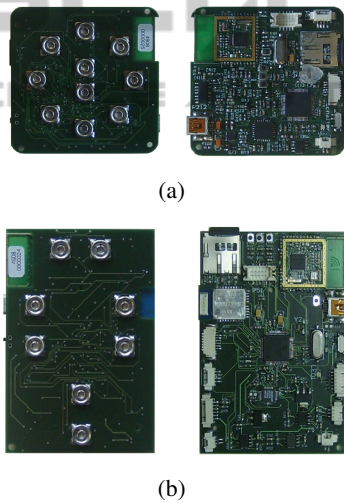


Figure 5: Implemented control modules of a) the sensor shirt, b) the cooling vest.

The snap fasteners on the textile material are connected to each other via isolated conductive yarns. In this prototype, ELITEX yarn (TITV, 2008), which comprises many silver coated polyamide filaments insulated by a polyurethane film, was used. It was sewn meander-shaped on the textile material and soldered at its ends to the snap fasteners before crimping these into the textile like in (Lamparth et al., 2009) (see Figure 3).

## 2.2 Regulation Algorithm

The conceived regulation algorithm is based on the measured vital and surroundings parameters and is shown in Figure 6.

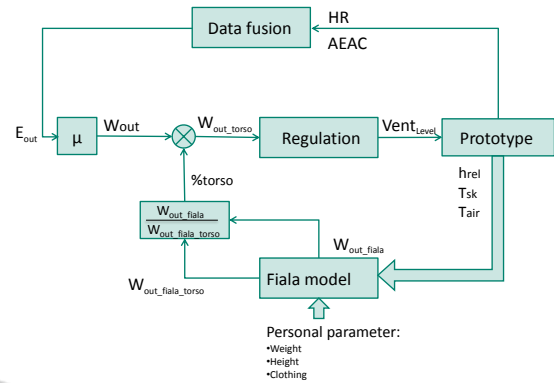


Figure 6: Knowledge based regulation algorithm.

In a first stage, the heart rate ( $HR$ ) and the activity equivalent for the acceleration ( $AEAC$ ), described in section 2.1.1, are fused in order to approximate the actual metabolic activity of the body.

Therefore, the sensor data is being post processed in order to avoid a strong fluctuation and thus an instability of the regulation algorithm. The  $HR$  values, which have been determined event-driven, are first filtered by a median filter having the width of 11 samples and then averaged over a moving window having the width of 5 samples. The  $AEAC$  values, which have been measured with a sample rate of 20 Hz, are only averaged over a moving window having the width of 30 samples. These settings have been determined after conducting two tests and have shown a good behavior with a minimal fluctuation and without causing an unacceptable reaction time of the system due to the resulting delays in the signals.

The data fusion model is shown in Figure 7.

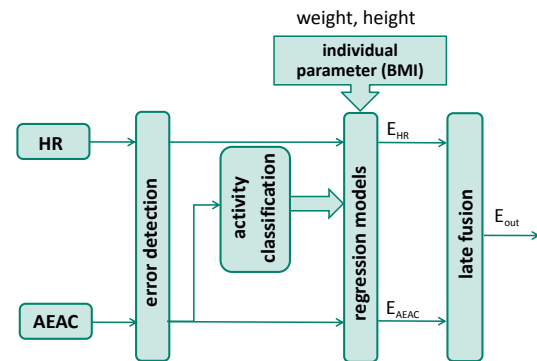


Figure 7: Data fusion model for approximating the metabolic activity of the body.

The error detection component filters outliers by means of a confidence interval analysis (for both  $HR$  and  $AEAC$ ). In this way, faulty measurements, which

can for instance be caused by an ECG electrode loosening contact with the skin due to a high activity dynamic, and a malfunction of a sensor can be compensated.

The data fusion model also integrates a decision tree based activity classification that classifies activity into two categories: low activity (e.g. laying, standing or walking slowly) and middle to high activity (e.g. walking fast or running). This classification is based on two features related to the *AEAC* signal; the value of *AEAC* itself and its variance. Since the classification algorithm is being implemented on a microcontroller, which has limited resources, the variance was approximated with an integral over the last 30 *AEAC* variations ( $\Delta AEAC$ ) according to formula 3.

$$AEAC_{int30} = \sum_{t-30}^t \Delta AEAC(t). \quad (3)$$

The results of the action analysis component are then used by activity based regression models that map the corresponding vital parameter (*HR* and *AEAC*) to a reference measurement of the metabolic activity (registered by a spirometer) by means of the robust least mean square method as adopted in (Rennie et al., 2000). At the same time, these regression models take into consideration the body mass index *BMI* (see equation 4) in order to minimize the approximation failure from one person to another.

$$BMI = \frac{weight_{body}[kg]}{(height_{body}[m])^2} \quad (4)$$

In this way, the polynomial equations 5 to 8, which approximate the energy expenditure of the body respectively from *HR* and *AEAC* for both states, low and high activities, have been determined.

$$E_{HR,low} = \alpha_{HR,low} \cdot HR + \beta_{HR,low} + \gamma_{HR,low} \cdot BMI \quad (5)$$

$$E_{HR,high} = \alpha_{HR,high} \cdot HR + \beta_{HR,high} + \gamma_{HR,high} \cdot BMI \quad (6)$$

$$E_{AEAC,low} = \alpha_{AEAC,low} \cdot AEAC + \beta_{AEAC,low} + \gamma_{AEAC,low} \cdot BMI \quad (7)$$

$$E_{AEAC,high} = \alpha_{AEAC,high} \cdot AEAC^3 + \beta_{AEAC,high} \cdot AEAC^2 + \gamma_{AEAC,high} \cdot AEAC + \delta_{AEAC,high} + \phi_{AEAC,high} \cdot BMI \quad (8)$$

The determined metabolic activities from *HR* and *AEAC* are then fused in order to approximate the actual metabolic activity of the body and thus get  $E_{out}$ .

Two fusion methods have been implemented: simple mean building and kalman filter.

After multiplying the determined metabolic activity  $E_{out}$  with the efficiency factor of approximately 20% (Fiala et al., 2001), the total amount of the generated body heat  $W_{out}$  that has to be released can be calculated.

Besides, the measured temperature and relative humidity of the skin, the aspirated air in the cooling vest and the person specific parameter (weight, height and clothing) are applied to a knowledge based model according to the fiala model (Fiala et al., 1999; Fiala et al., 2001). Thereby, the percentage of the body heat, which is released by the body under the cooling vest  $W_{out,torso}$  (torso area), can be approximated.

The actuating variable for the active climate control is the ventilation level  $Vent_{Level}$ . This latter is proportional to the rotation speed of the ventilators at the outlets of the cooling vest and is thus responsible for varying the airflow. The operating range of the used ventilators is linearly split up into 11 discrete levels:

Level 0 = ventilators are inactive

Level 1-9 = ventilators are active

Level 10 = maximal ventilation (corresponds to 100 L/min)

The calculated ventilation level ( $Vent_{Level}$ ) comprises two components: the ventilation level calculated from the measured sensor data and the determined body heat  $W_{out,torso}$  ( $Alg_{Level}$ ), and the user level ( $User_{Level}$ ), which is set online by the user via the PDA and thus gives him the possibility to fine tune the ventilation level according to his individual comfort feeling and even switch it off, if desired (see formula 9).

$$Vent_{Level} = Alg_{Level} + User_{Level} \quad (9)$$

$$with \ 0 \leq Vent_{Level} \leq 10$$

$$0 \leq Alg_{Level} \leq 10$$

$$-Alg_{Level} \leq User_{Level} \leq 10 - Alg_{Level}$$

The concept of the regulation component is shown in Figure 8. It uses the determined body heat  $W_{out,torso}$  and a knowledge based regression model from the data of the first field study. This way, the necessary airflow and thus the corresponding ventilation level can be calculated.

Since the metabolic activity, and especially the basal metabolic rate, varies from one person to another, a calibration phase has been implemented (as shown in Figure 8) in order to compensate the baseline body heat  $W_{baseline}$  corresponding to the basal metabolic rate. This calibration phase takes place in the first 30 seconds of the measurement cycle, where

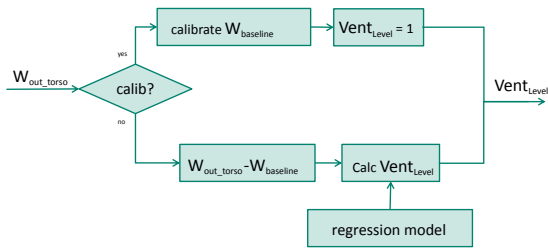


Figure 8: Calibration based regulation component.

the test person is inactive.  $W_{baseline}$  is calculated and averaged over the 30 seconds. After that, the offset of  $W_{baseline}$  is subtracted from the calculated released body heat  $W_{out\_torso}$ .

### 2.3 Field Study

The conducted field study aimed at collecting detailed information about the physiological interdependencies and their correlation with the workload. As a reference, the consumption of oxygen is saved by means of a spirometer during the load test. An offline analysis later on allows for validating the sensor data of the new prototype and adjusting the existing regression models for the calculation of the energy expenditure or metabolic activity of the body from the sensor data (Hollmann, 2006) according to the new design of the sensor shirt, in which the position of the acceleration sensor has changed and a new material of the ECG electrodes is used.

Besides, a verification of the suitability of the new prototype for the daily use and a validation of the implemented algorithm for active body climate control can be conducted.

Nine test persons (high school students, males) participated in the field study (see Table 1).

Table 1: Physiological data of the nine test persons.

	Mean value	Standard deviation
Age [years]	26,5	± 3,5
Height [cm]	182	± 8
Weight [kg]	81,25	± 12,25

**Field Study Procedure.** Each test person undertook a load test on a treadmill ergometer wearing the implemented prototype and a spirometer. The test procedure had to be conceived in a way that it makes it possible to compare the results of the load tests related to different test persons. Therefore, a low workload level in the beginning of the test and short workload phases, which do not exclude the reaching of a bio-physiological steady state status, needed

to be considered. According to (Wahlund, 1948), an absolute steady state status for light to middle workload is reached after 6 minutes. Investigations of the sports university in Koeln/Germany showed that 90 to 95% of the steady state status can be registered already after 3 minutes of the beginning of a constant workload (Knipping et al., 1953). For the conducted load test, a tradeoff was met analog to (Hollmann, 1963). After a baseline phase of 5 minutes, an intensity level of 6 km/h was set at the treadmill ergometer for the period of 5 minutes followed by an increase in the intensity level with 1 km/h. After the load test phase with the maximum intensity level of 10 km/h, the test person rested for 10 minutes. This baseline phase after the end of the load test enables the observation and the understanding of the relaxation behavior of the body.

**Test Person Feedback Form.** During the study, subjective feedback from the test persons was collected by means of a test person feedback form. This latter includes general questions before the beginning of the load test dealing with the performance anamnesis (general fitness, physical and mental state on the day of testing, feeling of the room climate, etc.) and recording the individual physiological data of each test person (e.g. age, body height, weight, etc.) and the climate in the room of the study (temperature, moisture, etc.). During the load test, the actual wearing comfort of the vest and the local thermal comfort at the chest and the back were registered in the middle of every phase of the test. After the end of the test, the test persons gave their feedback related to the absolved test and to the test settings (for instance the new prototype and the efficiency of its active climate control).

## 3 RESULTS AND DISCUSSION

### 3.1 Data Fusion

In order to assess the implemented data fusion algorithm, the Mean Absolute Percentage Error (MAPE) has been calculated according to equation 10 for all nine test persons, who took part in the field study.

$$MAPE = \frac{1}{n} \sum_{t=1}^n \left| \frac{y_t - x_t}{y_t} \right| \quad (10)$$

Thereby,  $y_t$  represents the reference value corresponding to the energy expenditure calculated from the spirometer data and  $x_t$  represents the estimated value from the sensor data ( $HR$  and  $AEAC$ ) in case

Table 2: MAPE for the nine test persons.

Test person	MAPE [%]
1	18.41
2	28.80
3	22.68
4	27.42
5	12.74
6	27.93
7	23.77
8	41.29
9	19.47
$\emptyset$	24.72

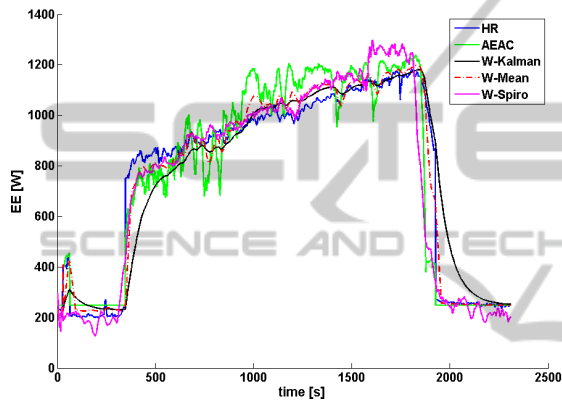
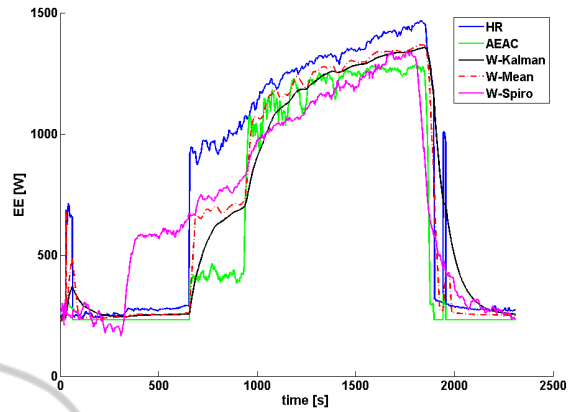


Figure 9: Comparison of the approximated metabolic activity with the spirometer data for test person №5.

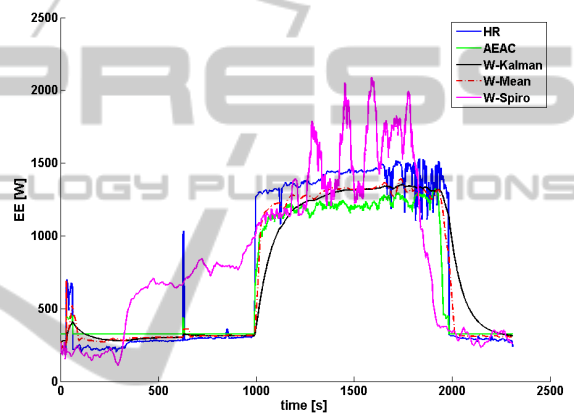
of fusion by the mean building method.

According to Table 2, the approximation of the metabolic activity for test persons №1, 5 and 9 was good, Figure 9 shows that for test person №5 exemplarily. In fact, the calculated metabolic activity (dashed red line) follows the reference measurement of the spirometer (magenta line) and has a small mean deviation of 12.74%. The fusion model, which uses kalman filter for the fusion of the calculated metabolic activities, (black line) has shown similar good results like the mean building method, except that it has a longer reaction time and thus a bigger time delay. Since the mean building method additionally needs less calculational resources than the kalman filter, it is more appropriate for online implementation on the microcontroller.

As for the other test persons, a stronger deviation from the spirometer data can be observed. This is due to incorrect activity classification in the data fusion model. In fact, the majority of the test persons were walking fast in the first load test phase between the 5<sup>th</sup> and the 10<sup>th</sup> minute (see Figure 10). But this was classified as a low activity rather than high activity and thus the metabolic activity was underestimated.



(a)



(b)

Figure 10: Comparison of the approximated metabolic activity with the spirometer data for a) test person №9, b) test person №8.

Test person №8 was walking fast even in the second load phase corresponding to 7 km/h. In addition his spirometer data (magenta line in Figure 10 b)) has shown an instability that led to the corresponding bad MAPE in Table 2. This can be explained by the fact that the test person lifted the mask of the spirometer during the load test in order to adjust it, which had an impact on the initial calibration of the spirometer and led to its malfunction.

### 3.2 Regulation Algorithm

In order to validate the implemented regulation algorithm, a comparison of the calculated ventilation level ( $Vent_{Level}$ ) and the ventilation level calculated from the measured sensor data and the determined body heat  $W_{out\_torso}$  ( $AlgLevel$  or  $Vent_{Level,theoretical}$ ) is necessary. Figure 11 shows the observed trend for the majority of the test persons.

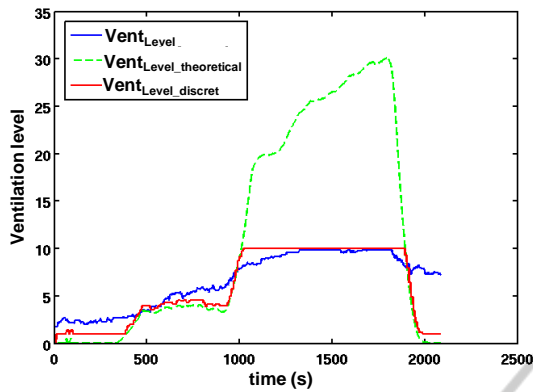


Figure 11: Comparison of the theoretical and the real ventilation level for a test person during the load test for test person №9.

One can see that the deviation is small during the load test until the load phase of 8 km/h. After that, the calculated ventilation level exceeds the maximal ventilation level, which corresponds to the maximal airflow in the cooling vest of around 100 L/min. This implies that the ventilation resources are not sufficient for relatively high loads. At the end of the load test during the second baseline phase (after the 30<sup>st</sup> minute), the theoretical ventilation level decreased rapidly. But the test person wanted more ventilation and has compensated it via the feedback channel of the PDA. This can be explained by the fact that the calculated metabolic activity has decreased rapidly at the beginning of the second baseline phase since the *AEAC* parameter decreased rapidly too. In other words, there is a need for taking the relaxation phase of the body after an important and lasting physical activity into consideration.

Figure 12 shows that the measured body heat  $W_{out\_vest\_total}$  (continuous red line), which is transported away by means of the airflow circulating within the cooling vest, is basically an evaporation heat ( $W_{out\_evap}$ ) and the convection part ( $W_{out\_conv}$ ) is very negligible. In addition, a comparison of the calculated released body heat at the torso area  $W_{out\_torso}$  (magenta line) and the measured heat  $W_{out\_vest\_total}$  (continuous red line) shows a gap between the two lines, which can reach 150 W. This can be explained by the fact that the actual ventilation resources are below the theoretically needed airflow. In addition, the absorption capacity of the textile material of the sensor shirt prevents the total amount of the released evaporation heat from getting into the ventilation layer.

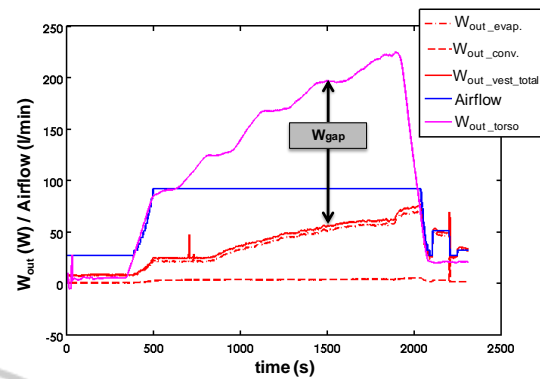


Figure 12: Comparison of the released body heat at the torso and the heat transported away within the cooling vest for test person №3.

## 4 CONCLUSIONS AND FUTURE WORK

The new prototype for active body climate control has shown better results than the previous design described in (Gharbi et al., 2010). Thereby, the different components of the implemented regulation algorithm have been validated with the data of the conducted field study. In addition, the test persons, who took part in the conducted field study, gave an overall positive feedback regarding the suitability of the new prototype for the daily use. They also confirmed the added value of the cooling system that actively supports their body thermoregulation. Nevertheless, some limitations of the current system and its algorithms could be identified and several enhancements need to be carried out:

The fusion model, especially the activity classification component, needs to be further optimized in order to get a more accurate estimation of the metabolic rate.

As for the regulation algorithm, the relaxation phase of the body after an important and lasting physical activity needs to be modeled, so that an appropriate ventilation level close to the subjective optimum of the wearer of the system can always be guaranteed.

Concerning the presented prototype for active body climate control, the design of the ventilation area of the cooling vest needs to be improved, so that the ventilation resources would be sufficient for high workloads. For that, new designs of the space holder material need to be investigated in order to reduce the air resistance inside the cooling vest. Another alternative is the integration of more than two ventilators in the cooling vest and/or the selection of more powerful ventilators.

## ACKNOWLEDGEMENTS

This work is done in the framework of the joint research project "KlimaJack", which is financed by the German ministry for education and research. Besides the Institute for Information Processing Technology (KIT), other German industrial parties (Beurer, IMST, Lodenfrey, MVS and Ruhlamat) have contributed to the conducted research work.

## REFERENCES

- Crawshaw, L. I., Nadel, E. R., Stolwijk, J. A. J., and Stamford, B. (1975). Effect of local cooling on sweating rate and cold sensation. *Pflgers Archiv: European Journal of Physiology*, 354:19–27.
- Fiala, D., Lomas, K., and Stohrer, M. (1999). A computer model of human thermoregulation for a wide range of environmental conditions: The passive system. *Journal of Applied Physiology*, 87:1957–1972.
- Fiala, D., Lomas, K., and Stohrer, M. (2001). Computer prediction of human thermoregulatory and temperature responses to a wide range of environmental conditions. *International Journal of Biometeorology*, 45:143–159.
- Gharbi, A., Kraehling, C., Stork, C., and Mueller-Glaser, K. D. (2010). Evaluation system for monitoring of vital parameters and active body climate control. In *Biosignals: 3rd International Conference on Bio-inspired Systems and Signal Processing*. INSTICC Press.
- Hollmann, W. (1963). *Hoechst- und Dauerleistungsfähigkeit des Sportlers*. Barth, Munich.
- Hollmann, W. (2006). *Spiroergometrie : kardiopulmonale Leistungsdiagnostik des Gesunden und Kranken*. Schattauer, Stuttgart.
- IMST GmbH (2009). WiMOD - iM221A Datasheet: low power radio module for the 2.4 GHz ISM band.
- Jatob, L., Gromann, U., Ottenbacher, J., Haertel, S., von Haaren, B., Stork, W., Mueller-Glaser, K., and Boes, K. (2007). Obtaining energy expenditure and physical activity from acceleration signals for context-aware evaluation of cardiovascular parameters. In *CLAIB*.
- Knipping, H., Albrecht, H., Valentin, H., and Venrath, H. (1953). Ueber die atmung und das herzminutenvolumen bei arbeit und sport, sowie die herzleistung. *Zeitschrift für die gesamte experimentelle Medizin*, 122:356–368.
- Lamparth, S., Fuhrhop, S., Kirst, M., Wagner, G. v., and Ottenbacher, J. (2009). A mobile device for textile-integrated long-term ecg monitoring. In *IFMBE Proceedings: World Congress on Medical Physics and Biomedical Engineering, Munich, Germany*.
- Microchip Technology Inc. (2010). PIC24FJ256GB110 family Datasheet: 16 bit RISC microcontroller.
- MITSUMI ELECTRIC CO., LTD. (2010). WML-C46 Datasheet: Bluetooth module, class 2.
- Olesen, B. W. and Fanger, P. O. (1973). The skin temperature distribution for resting man in comfort. *Pflgers Archiv: European Journal of Physiology*, 27:385–393.
- Rennie, K., Rowsell, T., Jebb, S. A., and Holdurn, D. (2000). A combined heart rate and movement sensor proof of concept and preliminary testing study. *European Journal of Clinical Nutrition*, 54:409–414.
- Silbernagl, S. and Despopoulos, A. (2003). *Taschenatlas Physiologie*. Thieme ElectronicBook Library. Thieme, Stuttgart [u.a.], 6., vollst. bearb. und erw. aufl. edition.
- TITV (2008). ELITEX Datasheet: conductive yarn.
- Wahlund, H. (1948). Determination of the physical working capacity. *Acta Medica Scandinavica*, 132:1–78.